The effect of crack length on the fracture parameters of an edge crack parallel to the material variation in a rectangular FGM plate

Haider Khazal Mehbes

Hassanein Ibraheem Khalaf

Ameen Ahmed Nasser

Mechanical Engineering Department, Basrah University, Basrah, Iraq

Abstract. In this study, the extended element free Galerkin method (XEFG) is used for crack analysis an edge crack parallel to the material variation in a rectangular functionally graded material (FGM) plate under traction loading. For the first time, the effective parameters of XEFGM are employed such as the sub-triangulation term for numerical integration, suitable influence domain, and enrichment functions for discontinues locations in the fracture analysis of different crack positions of an edge cracked FGM plate. In addition, the incompatible formulation is adopted to extract the stress intensity factors (SIFs). Good data and results are observed about the relationship between the crack lengths and SIFs with good verification during changing XEFG parameters. There is good agreement and stability in the results of SIFs through the sizes of J-integral rJ equal to 0.4 -0.8. In addition, the acceptance results for the size of the support domain are bound between dmax=1.52 to 2.

Keywords: extended element free Galerkin method; crack length, functionally graded materials; stress intensity factors

NOMENCLATURE

Symbol	Description	Unit
E	Modulus of elasticity (Young's Modulus)	MPa
G	Shear modulus	MPa
M	Interaction integral	N/m
N	number of nodes	…….
a	The length of a crack	mm
b	Body force	N
d_{mI}	variation of the support domain	m
n	Number of nodes in the influence of domain	…….
n_j	The unit outward normal to contour	…….
r	Radial distance from a crack tip	m
rJ	Size of J-Inegral	m
$\bar{t}$	traction force	N
t	Time	s
u^h	The unknown trial approximation of displacement	m
$\bar{u}$	The prescribed displacements on the boundary	m
w	The weight function of an influence node	…….

Ω	The global domain of the problem	…….
Γ	Boundary of the global domain	…….
δ	Kronecker delta	…….
ϕ	Shape function	…….
ν	Poisson's ratio	…….
κ	Kolosov constant	…….
ρ	Mass density	kg/m^3
λ	Lagrange multiplier	…….

1. Introduction

In the recent decades, there are many applications for functionally graded materials (FGMs) in the engineering fields, involving military usages, space vehicle, electrical insulator, bio-medical, etc. According to the literature survey, the fracture analysis of FGMs was studied by many of researchers using the conventional and advanced numerical methods as the finite element method (FEM) [1-4], boundary element method [5], meshfree methods [6-10], and extended finite element method (XFEM) [11-15]. Most of the mentioned references focused on the employed of the numerical methods to extract the stress intensity factors at fixed crack tip position. The study of the effect of the crack length or crack size in certain materials not FGM was done by some of researchers as depicted in [16-19]. These studies were important to know the strength ranges of the related materials against the fracture, and to understand the critical fractures parameters and terms for the whole domain. However, the effect of the crack length on the fracture terms such as SIFs is unadulterated interest in this research. In the particular, lately, Khazal et al. [6] adopted an extended element free Galerkin method (XEFGM) for extract SIFs in one crack position in a rectangular FGM plate, therefore this paper will extend the investigation of the effect of the discontinuity length on the fracture parameters by using XEFGM. In addition, verification is employed between the results obtained by the present study and available references solutions in the literature. Hence, this study will report the effect of crack lengths on the fracture parameters of a functionally graded material numerically. The incompatible interaction integral method will use to determine the fracture parameters as SIFs. In addition, the effective parameters of XEFGM will employ such as the sub-triangulation term for numerical integration, suitable influence domain, and enrichment functions for discontinues locations in the fracture analysis of different crack positions of an edge cracked FGM plate.

2. Displacement and Stress Field Equations

Referring to Hook's law, the strain can be written as follow:

$$\varepsilon = C\sigma = \begin{bmatrix} C_{11} & C_{12} & C_{16} \\ C_{12} & C_{22} & C_{26} \\ C_{16} & C_{26} & C_{66} \end{bmatrix} \begin{Bmatrix} \sigma_{xx} \\ \sigma_{yy} \\ \sigma_{xy} \end{Bmatrix} \quad (1)$$

where C is the compliance matrix. In FGM as illustrated in Figure 1, the material traits such as the Young modules Y and the Poisson's ratio ν, change referring to:

$$Y = Y(x_1, x_2) = Y(x), \upsilon = \upsilon(x_1, x_2) = \upsilon(x) \quad (2)$$

In addition, the singular stress field (σ) and displacement field in the terms of the standard angular functions at the crack location can be written as [20]:

$$\sigma_{11} = \frac{1}{\sqrt{2\pi r}} [K_I f_{11}^I(\theta) + K_I f_{11}^{II}(\theta)] \quad (3)$$

$$\sigma_{22} = \frac{1}{\sqrt{2\pi r}}[K_I f_{22}^I(\theta) + K_{II} f_{22}^{II}(\theta)] \quad (4)$$

$$\sigma_{12} = \frac{1}{\sqrt{2\pi r}}[K_I f_{12}^I(\theta) + K_{II} f_{12}^{II}(\theta)] \quad (5)$$

$$u=\{u_1, u_2\}T \quad (6)$$

$$u_1 = \frac{1}{G_{tip}}\sqrt{\frac{r}{2\pi}}[K_I g_1^I(\theta) + K_{II} g_1^{II}(\theta)] \quad (7)$$

$$u_2 = \frac{1}{G_{tip}}\sqrt{\frac{r}{2\pi}}[K_I g_2^I(\theta) + K_{II} g_2^{II}(\theta)] \quad (8)$$

$$G_{tip} = \frac{Y_{tip}}{[2(1+\nu_{tip})]} \quad (9)$$

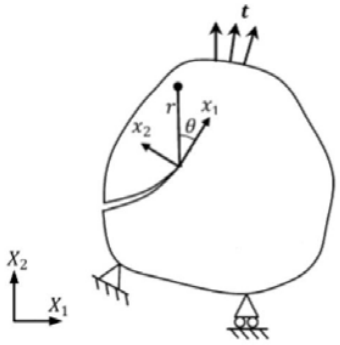

Figure 1: A cracked FGM domain.

3. XEFGM Procedure

Figure 2 depicts 2D problem of fracture problem that includes a crack $\boldsymbol{\Gamma_c}$. For this issue, the PD equation can be defined in the form of equilibrium equation as [6]:

$$\boldsymbol{L^T\sigma + b = 0} \quad in\ problemd\ dmain\ \Omega \quad (10)$$

where L is the differential operator written as

$$L = \begin{bmatrix} \frac{\partial}{\partial x} & 0 \\ 0 & \frac{\partial}{\partial y} \\ \frac{\partial}{\partial y} & \frac{\partial}{\partial x} \end{bmatrix} \quad (11)$$

and $\boldsymbol{\sigma, b}$ and $\boldsymbol{u}$ are the stress, body force, and displacement vectors, respectively. EFGM adopts moving least squares (MLS) technique [21] that put the shape functions to be worked totaly in the terms of distributed nodes. The weak form of the governing equation can be defined as[6]:

$$\int_\Omega (\boldsymbol{L\delta u})^T(\boldsymbol{DLu})d\Omega - \int_\Omega \delta\,\boldsymbol{u}^T\boldsymbol{b}d\Omega - \int_{\Gamma_t}\delta\,\boldsymbol{u}^T\bar{\boldsymbol{t}}d\Gamma - \int_{\Gamma_u}\delta\,\boldsymbol{\lambda}^T(u-\bar{u})d\Gamma - \int_{\Gamma_u}\delta\,\boldsymbol{u}^T\lambda d\Gamma = 0 \quad (12)$$

where $\boldsymbol{\lambda}$ represents the Lagrange multiplier variable.

The displacement form that extract from the governing equation by applying XEFGM can be written as:

$$\boldsymbol{u}^h(\boldsymbol{x}) = \sum_{i=1}^{n} \phi_i(\boldsymbol{x})\boldsymbol{u}_i + \sum_{k=1}^{s_t} \phi_k \sum_{\alpha=1}^{4} E_\alpha(\boldsymbol{x})\boldsymbol{b}_k \quad (13)$$

where $\boldsymbol{b}_k$ represents extra DOFs that add crack tips, s_t is the nodes which the discontinuity in its support domain, and $E_\alpha(\mathbf{x})$ are the enrichment functions [6, 22]:

$$E(r,\theta) = \left(\sqrt{r}\cos\left(\frac{\theta}{2}\right), \sqrt{r}\sin\left(\frac{\theta}{2}\right), \sqrt{r}\sin\left(\frac{\theta}{2}\right)\sin(\theta), \sqrt{r}\cos\left(\frac{\theta}{2}\right)\sin(\theta)\right) \quad (14)$$

Discretization of Eq. (12) defines:

$$\begin{bmatrix} \boldsymbol{K} & \boldsymbol{Q} \\ \boldsymbol{Q}^T & \boldsymbol{0} \end{bmatrix} \begin{bmatrix} \boldsymbol{U} \\ \boldsymbol{\lambda} \end{bmatrix} = \begin{bmatrix} \boldsymbol{F} \\ \boldsymbol{q} \end{bmatrix} \quad (15)$$

where $\boldsymbol{K}$ represents the global stiffness matrix, $\boldsymbol{F}$ defines as the global force vector, $\boldsymbol{Q}$ and $\boldsymbol{q}$ are the Lagrange related terms for enforcement of the boundary conditions by the Lagrange multipliers $\boldsymbol{\lambda}$ [6]. In a particular, suitable election for the influence domain near a crack tip is adopted which is depended on the similar method used in FGMs crack examples by [6,23].

For the numerical integrations of the relevant equations, Gauss quadrature method is applied thru the background cell of XEFGM. The background cell that existed with a crack is divided at both sides into sub-triangles that edges are used to the crack surfaces. Gauss quadrature that uses a background structure and uniform nodal distribution are used in the modeling of the numerical examples. More details for the representation of the Gauss quadrature method and sub-triangles technique can be viewed in [23].

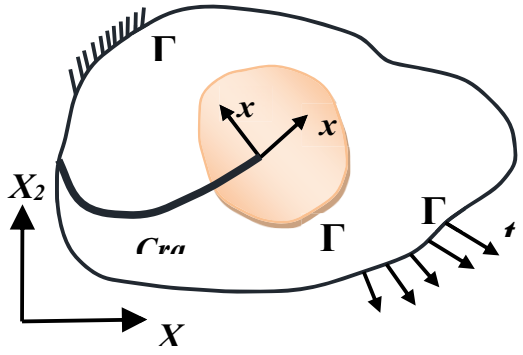

Figure 2: A 2D fractured domain.

4. Calculation of SIFs by the interaction integral method

The incompatibility formulation is followed for the auxiliary fields of cracked body [2,6]:

$$\sigma_{ij} = y_{ijkl}(x)\varepsilon_{kl} \ , \quad \varepsilon_{ij} \neq \frac{1}{2}\left(u_{i,j} + u_{j,i}\right) \ , \ \sigma_{ij,j} = 0 \quad (16)$$

The equivalent domain equation of the J-integral of Γ around the crack tip represents as (Figure 3):

$$J = \int_A \left(\sigma_{ij}u_{i,1} - w\delta_{1j}\right)q_{,j}\, dA + \int_A \left(\sigma_{ij}u_{i,1} - w\delta_{1j}\right)_{,j} q dA \quad (17)$$

where w represents the strain energy density:

$$w = \frac{1}{2}\sigma_{ij}\varepsilon_{ij} \tag{18}$$

The incompatibility formulation is implemented to find the mode I and II SIFs :

$$M = \int_A \left\{\sigma_{ij}u_{i,1}^{aux} + \sigma_{ij}^{aux}u_{i,1} - \frac{1}{2}(\sigma_{ik}u_{ik}^{aux} + \sigma_{ik}^{aux}u_i)\delta_{1j}\right\}q_{,j}\,dA + \int_A \left\{\sigma_{ij}\left(c_{ijkl}^{tip} - c_{ijkl}(x)\right)\sigma_{kl,1}^{aux}\right\}q dA \tag{19}$$

Therefore, J-integral can be written in terms of mode I and mode II SIFs:

$$J_{local} = (K_I^2 + K_{II}^2)/E_{tip} \tag{20}$$

$$J_{local}^s = \frac{\left(K_I + K_I^{aux}\right)^2 + \left(K_{II} + K_{II}^{aux}\right)^2}{Y_{tip}} = J_{local} + J_{local}^{aux} + M_{local} \tag{21}$$

Where Jlocal drived by Eq. (20), and J_{local}^{aux} represent by

$$J_{local}^{aux} = [(K_I^{aux})^2 + (K_{II}^{aux})^2]/Y_{tip} \tag{22}$$

and M_{local} is

$$M_{local} = 2(K_I K_I^{aux} + K_{II}K_{II}^{aux})\ /Y_{tip} \tag{23}$$

The mode I and mode II SIFs are extracted as gives:

$$K_I = M_{local}^{(1)}Y_{tip}\ /2\,, \qquad (K_I^{aux} = 1.0\,, K_{II}^{aux} = 0.0),$$

$$K_{II} = M_{local}^{(2)}Y_{tip}\ /2\,, \qquad (K_I^{aux} = 0.0\,, K_{II}^{aux} = 1.0). \tag{24}$$

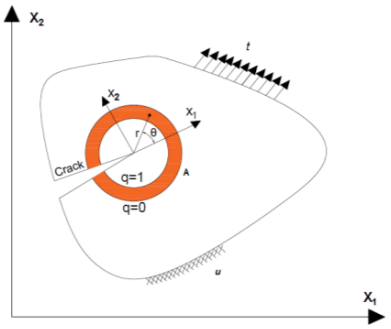

Figure 3: The model of contour at the tip of discontinuity .

5. Numerical case study

An edge crack FGM plate under traction load is adopted as shown in Figure 4. The change of the material properties is in the x1- direction according to the following equation:

$$Y(x1) = Yo\ e^{\alpha\, x1}, \alpha = \frac{1}{b}\ln\left(\frac{Yw}{Yo}\right) \quad (25)$$

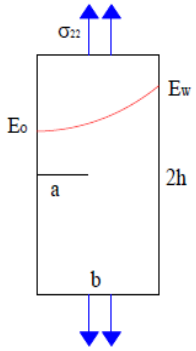

Figure 4: An edge crack FGM plate (b= 10 mm, 2h = 30 mm, ν=0.25).

Where Y0=10000 MPa and Yw=50000 MPa are the Young's modulus at the left and right side of the plate, respectively. Circular support domain in term of cubic spline weight function with linear basis function are employed. Uniform distribution nodes, and background cells with Gauss quadrature term in each cell are adopted. Total number of nodes and background cells are 1624 and 1479 respectively. Total enrichment nodes in the crack tip are 64 node (16×4). The integration of the numerical equation is done by a 2×2 Gauss quadrature rule in all cell except at the crack sub-triangle cells is adopted by 13 Gauss nodes. Figures 5 and 6 represent the geometry and numerical model of XEFGM.

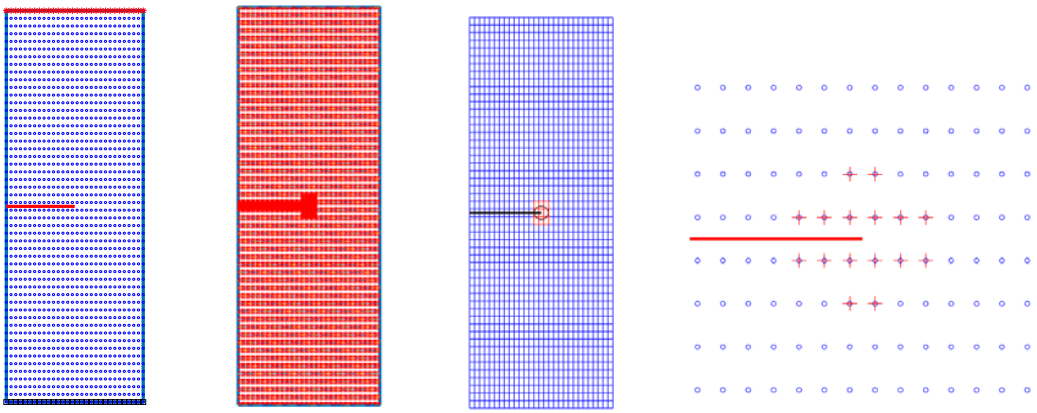

(a) (b) (c) (d)

Figure 5: (a) nodal distribution, (b) Gauss points, (c) background cell, and (d) enrichment nodes of the numerical model of an edge crack FGM plate (clack length a=5 mm).

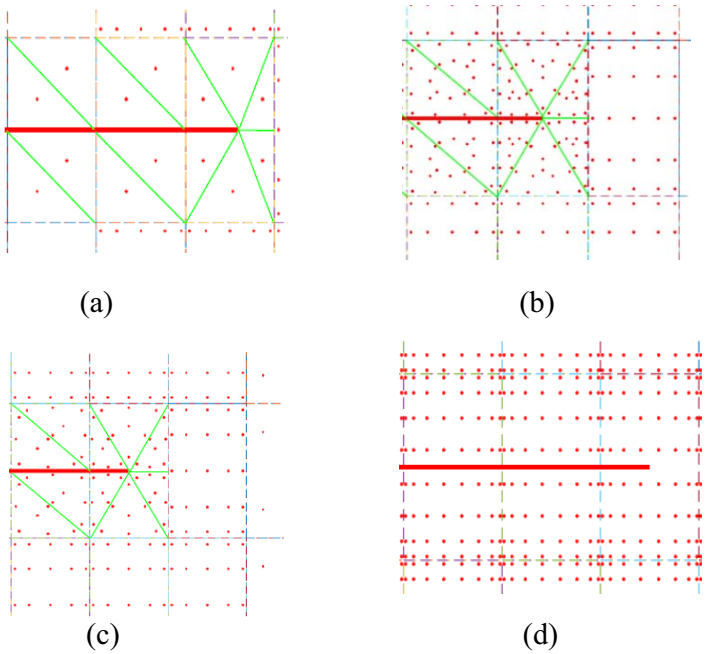

Figure 6. (a) 1 Gauss point for each proposed sub-triangle, (b) 13 Gauss points for each proposed sub-triangle, (c) 7 Gauss points for each proposed sub-triangle, and (d) 16 Gauss points of the standard approach of the numerical model in the crack region.

Table 1 compares the values of normalized SIFs in terms of crack lengths of the current work. For the verification issue, the work is compared with [5] at crack length equals to 4 mm because [5] have result only for this length only that used boundary element method. The error of the XEFG method with [5] can be viewed in Table 2. There is good agreement and stability in the results of SIFs through the sizes of J-integral rJ equal to 0.4 -0.8.

Table 1 Normalized SIFs (KI) of the present work in terms of the size of the J-integral domain (rJ) at size of support domain dmax=1.7 with 13 Gauss points for each sub-triangle.

a	$r_J = 0.4$	$r_J = 0.5$	$r_J = 0.6$	$r_J = 0.7$	$r_J = 0.8$	$r_J = 0.9$	$r_J = 1$	[5]
1	0.82388	1.0446	1.0446	1.0446	1.0502	1.0581	1.0768	-
2	0.70708	1.1816	1.1636	1.1479	1.1479	1.1598	1.1923	-
3	1.4034	1.4034	1.3818	1.3892	1.3892	1.3994	1.4646	-
4	1.7566	1.7566	1.7385	1.7681	1.7681	1.7873	1.8587	1.741
5	2.351	2.351	2.4041	2.4041	2.4041	2.4848	2.5095	-
6	3.5226	3.5226	3.5372	3.5206	3.5206	3.607	3.687	-
7	5.7538	5.7538	5.8018	5.7968	5.7968	5.9481	6.1907	-
8	9.6987	11.5217	11.8456	11.9466	11.9466	12.2571	12.7251	-
9	35.7161	42.3974	42.3974	42.3974	44.673	44.6849	46.7381	-

Table 2 The error of Normalized KI in comparing with [5] for $r_J = 0.5$, dmax=1.7, 13 Gauss points for each sub-triangle at a= 4 mm.

r_J	XEFG Normalized KI	Normalized KI [5]	Error %
0.4	1.7566	1.741	0.90
0.5	1.7566	1.741	0.90
0.6	1.7385	1.741	0.14
0.7	1.7681	1.741	1.56
0.8	1.7681	1.741	1.56
0.9	1.7873	1.741	2.66
1	1.8587	1.741	6.76

Table 3 shows the efficiency of the present technique (the sub-triangle technique) of the Gauss points distribution to calculate the correct SIF against standard approach. To further clarify Figure 6-a gives acceptance results for normalized KI at 1 Gauss point for each sub-triangle in comparing with standard approach 8×8 Gauss points. The best results can be determined at 7 and 13 Gauss points for each sub-triangle at the crack region as depicted in Table 4.

Table 3 Normalized SIFs (KI) of the present work in terms of various Gauss points in each cell in the crack region at dmax=1.7 with rJ=0.5.

a	Normalized KI at 1 Gauss point for each sub-triangle	Normalized KI at 7 Gauss points for each sub-triangle	Normalized KI at 13 Gauss points for each sub-triangle	Normalized KI at standard approach 4×4 Gauss points	Normalized KI at standard approach 8×8 Gauss points	Normalized KI [5]
1	1.0377	1.0441	1.0446	0.99138	0.99961	-
2	1.1422	1.1800	1.1816	1.0547	1.0805	-
3	1.3149	1.4005	1.4034	1.2883	1.3075	-
4	1.5835	1.7563	1.7566	1.5983	1.678	1.741
5	2.0243	2.3455	2.351	2.141	2.2965	-
6	2.9779	3.5006	3.5226	3.4958	3.5109	-
7	4.7191	5.7405	5.7538	6.0703	6.0671	-
8	9.9591	11.5894	11.5217	13.1671	12.613	-
9	56.7955	42.7133	42.3974	55.901	48.4083	-

Table 4 The error in Normalized KI in comparing with [5] for various number of Gauss points in each cell in the region of crack at crack length a=4 mm, and dmax=1.7 with rJ=0.5.

Gauss points distribution	XEFG Normalized KI	Normalized KI [5]	Error %
1 Gauss point for each sub-triangle	1.5835	1.741	9.04
7 Gauss points for each sub-triangle	1.7563	1.741	0.87
13 Gauss points for each sub-triangle	1.7566	1.741	0.89
standard approach 4×4 Gauss points	1.5983	1.741	8.19
standard approach 8×8 Gauss points	1.678	1.741	3.61

In addition, Figure 7 clears that the SIF increases when the crack length increases. The SIF at crack lengths equals to 9 mm is huge due to the plate reaches to the break as depicted in Figure 8.

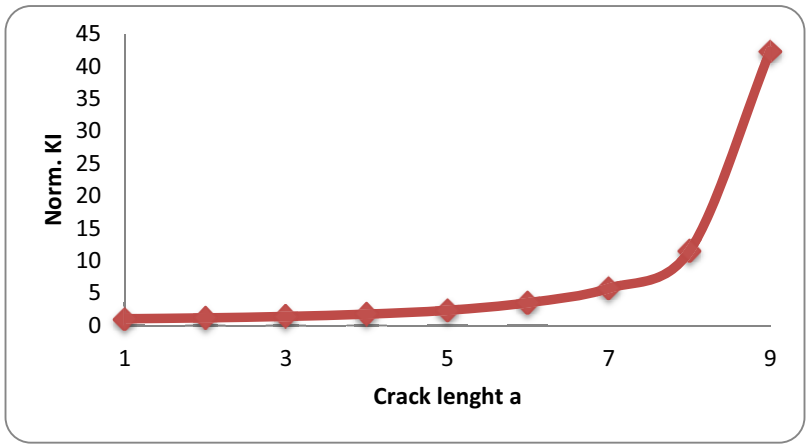

Figure 7: Values of normalized KI for various crack length at dmax=1.7, rJ=0.5, and 13 Gauss points for each sub-triangle.

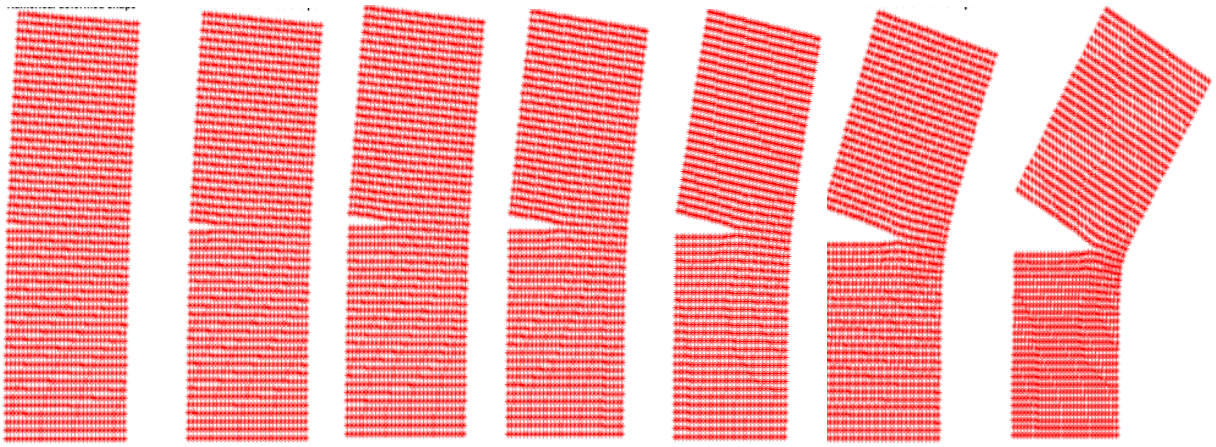

Figure 8: The deform shape of an edge cracked plate at crack lengths (a=1 to 7 mm).

Figure (9) illustrates the result of SIFs in terms of a number of nodes and background cells. Therefore, optimal background cell has to be chosen to avoid unnecessary computational costs with giving the same accuracy. In addition, meshfree methed has been good agreement, convergence, and stability against change the total number of background cells.

Hence, Figure (*10*) is given to depict the influence of size of support domain on the precision of normalized KI. The acceptance results are bound between dmax=1.52 to 2. The best result of SIFs is at dmax=1.52 to 1.7. It is clear that when the size of the support domain more than 2, the results of SIFs is not well convergence. Finally, despite the change in properties of the material through the x-axis, as illustrated in Figure (10), exceedingly regular stress contours are extracted without any stress extrapolation or stress refine methods. It is also obviously cleared that the right side from the plate seems higher σ_{yy} stress, due to intense stiffness, where Yw/Y0 is more than 2.5.

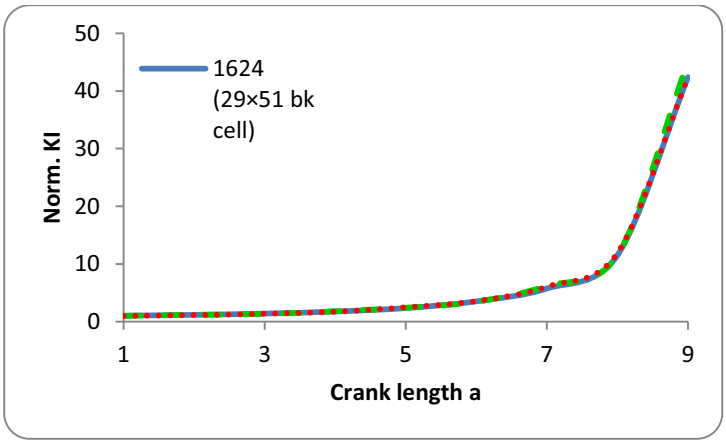

Figure 9: Values of normalized KI for various crack length at different number of nodes (dmax=1.7, rJ=0.5, and 13 Gauss points for each sub-triangle).

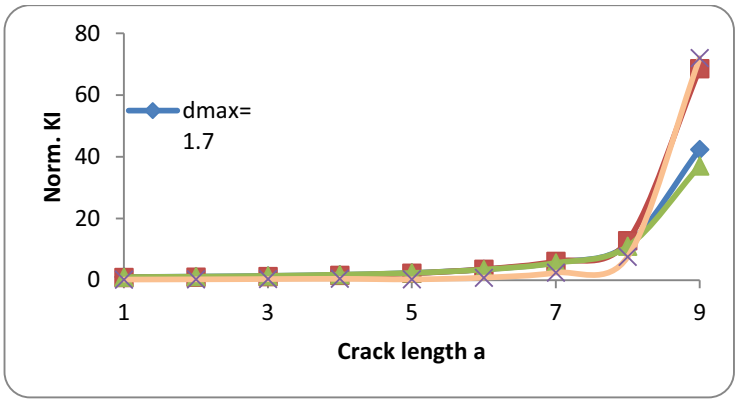

Figure 10: Values of normalized KI in terms of crack lengths at different sizes of support domain (rJ=0.5, and 13 Gauss points for each sub-triangle).

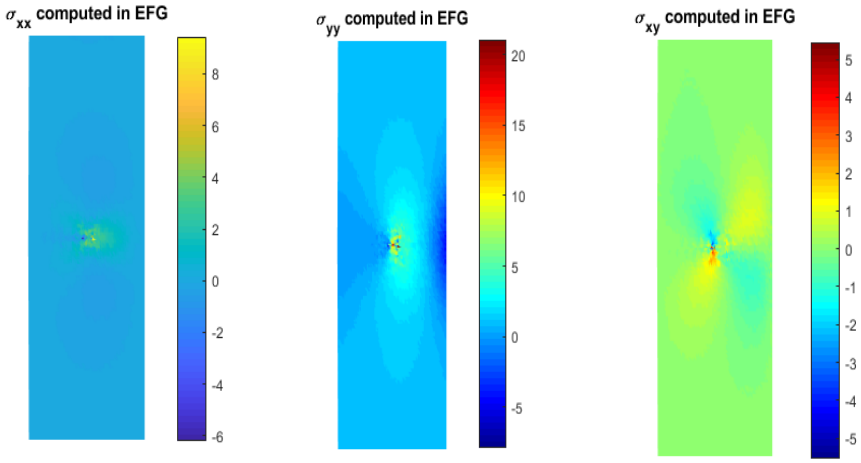

Figure 11: Stress contours of an edge cracked FGM plate under tensile loading (rJ=0.5, dmax=1.7, 13 gauss points for each sub-triangle)

6. CONCLUSIONS

This study reports the effect of crack lengths on the fracture parameters of a functionally graded material numerically and major conclusions of this study can explain in the following points:

1-The incompatible interaction integral method was used to determine the fracture parameters as SIFs.
2- The effective parameters of XEFGM were employed such as the sub-triangulation term for numerical integration, suitable influence domain, and enrichment functions for discontinues locations in the fracture analysis of different crack positions of an edge cracked FGM plate.
3- SIF in the plate increased when the crack length increased. The SIF at crack lengths equals to 9 mm is huge due to the plate reached to the break. In addition, in Gauss quadrature rule, the utilize of the sub- triangulation technique was given best results with good verification and stability with less integration points in comparing with the standard approach.
4- There is good agreement and stability in the results of SIFs through the sizes of J-integral rJ equal to 0.4 - 0.8.
5- The acceptance results for the size of the support domain are bound between dmax=1.52 to 2.

References

[1] J.-H. Kim and G.H. Paulino, On fracture criteria for mixed-mode crack propagation in functionally graded materials, Mechanics of Advanced Materials and Structures, vol.14, pp.227–244, 2007.

[2] J.-H. Kim and G. H. Paulino, Consistent formulations of the interaction integral method for fracture of functionally graded materials, Journal of Applied Mechanics, ASME, vol. 72, pp. 351-364, May 2005.

[3] J.-H. Kim and G.H. Paulino, Mixed-mode fracture of orthotropic functionally graded materials using finite elements and the modified crack closure method, Engineering Fracture Mechanics, vol.69 (14–16), pp.1557–1586, 2002.

[4] J. H. Kim, and G. H. Paulino, “Mixed mode crack propagation in functionally graded materials”, Ph.D thesis, University of Illinois at Urbana-Campaign, 2000.

[5] X.W. Gao, Ch. Zhang, J. Sladek and V. Sladek, “Fracture analysis of functionally graded materials by a BEM” Composites Science and Technology 68 (2008) 1209-1215.

[6] H. Khazal, H. Bayesteh, S. Mohammadi, Sayyed Shahram Ghorashi, and Ameen Ahmed, An extended element free Galerkin method for fracture analysis of functionally graded materials, Mechanics of Advanced Materials and Structures, vol.23, pp.513-528, 2016.

[7] S. Garg and M. Pant, “Numerical simulation of adiabatic and isothermal cracks in functionally graded materials using optimized element-free Galerkin method”, Journal of Thermal Stresses, Taylor and Francis 2017 .

[8] H. Khazal, and N. Saleh, “XEFGM for crack propagation analysis of functionally graded materials under mixed-mode and non-proportional loading”, Mech. Adv. Mater. Struct., vol. 0,1-9 2018. Doi: 10.1080/15376494.2018.1432786.

[9] J. Sladek, V. Sladek, and C. Zhang, “A meshless local boundary integral equation method for dynamic anti-plane shear crack problem in functionally graded materials”, Eng. Anal. Bound. Elem., vol. 29, pp. 334–342, 2005.

[10] W. Farouq, H. Khazal, and A. F. Hassan, "Fracture analysis of functionally graded material using digital image correlation technique and extended element-free Galerkin method", Optics and Lasers in Engineering, volume 121, October 2019, Pages 307-322

[11] J. Dolbow, “An extended finite element method with discontinuous enrichment for applied mechanics”, Ph.D. thesis, Northwestern University, Evanston, IL, USA, 1999.

[12] H. Bayesteh and S. Mohammadi, "XFEM fracture analysis of orthotropic functionally graded materials, Composites, Part B 44, pp.8–25, 2013.

[13] S.S. Hosseini, H. Bayesteh and S. Mohammadi, Thermo-mechanical XFEM crack propagation analysis of functionally graded materials, Materials Science and Engineering, vol. 561, no.20, pp. 285–302, January 2013.

[14] J. Dolbow, An extended finite element method with discontinuous enrichment for applied mechanics, Ph.D. thesis. Northwestern University, Evanston, IL, USA, 1999.

[15] A. Bergara, J. I. Dorado, A. Martín-Meizoso and J. M. Martínez-Esnaola," Fatigue crack propagation at aeronautic engine vane guides using the extended finite element method (XFEM)", Mechanics of Advanced Materials and Structures, 11 Apr 2019.

[16] K. Ando, B. A. Kim, M. C. Chu, and S. Sato, "effects of crack length, notch root radius and grain size on fracture toughness of fine ceramics", FFEMS,Volume16, Issue9,September 1993,Pages 995-1006.

[17] J. Akbardoost, "Size and crack length effects on fracture toughness of polycrystalline graphite", Engineering Solid Mechanics 2 (2014) 183-192.

[18] H. Khazal, A. Hassan, W. Farouq, and H. Bayesteh, "Computation of Fracture Parameters in Stepwise Functionally Graded Materials Using Digital Image Correlation Technique," Materials Performance and Characterization 8, no. 1 (0): 344-354.

[19] A.Turnbull, and L.Wright,"modelling the electrochemical crack size effect on stress corrosion crack growth rate", corrosion science, volume 126, September 2017, Pages 69-77.

[20] B.N. Rao and S. Rahman, Mesh-free analysis of cracks in isotropic functionally graded materials, Engineering Fracture Mechanics, vol.70 pp.1–27, 2003.

[21] P. Lancaster and K. Salkauskas, Surfaces generated by moving least squares methods, Mathematics of Computation, vol. 37, pp. 141-158, 1981.

[22] M. Fleming, Y. Chu, Moran B, T. Belytschko, Enriched element-free Galerkin methods for crack tip fields, Int J Numer Methods Engng,1997;40:1483–504.

[23] S.S. Ghorashi, S. Mohammadi and S.R.S. Yazdi , “Orthotropic enriched element free Galerkin method for fracture analysis of composites” Engineering Fracture Mechanics-Volume 78, Issue 9, June 2011, Pages 1906–1927.